J. Biochem. 2011;150(2):173–181 doi:10.1093/jb/mvr051

JB THE JOURNAL OF BIOCHEMISTRY

# Kinetic analysis of reactive oxygen species generated by the in vitro reconstituted NADPH oxidase and xanthine oxidase systems

*Received February 6, 2011; accepted March 27, 2011; published online May 13, 2011*

**Emiko Sato*, Takayuki Mokudai, Yoshimi Niwano and Masahiro Kohno**

New Industry Creation Hatchery Center, Tohoku University, 6-6-10 Aoba, Aramaki, Aoba-ku, Sendai 980-8579, Japan

*Emiko Sato, Tohoku University Graduate School of Pharmaceutical Sciences, 2-1 Seiryo-cho, Aoba-ku, Sendai 980-8575, Japan, Tel: +81 22 717 7163; Fax: +81 22 717 7168; e-mail: emiko@med.tohoku.ac.jp

**The nicotinamide adenine dinucleotide (NADH)/nicotinamide adenine dinucleotide phosphate (NADPH) oxidase and the xanthine oxidase (XOD) systems generate reactive oxygen species (ROS). In the present study, to characterize the difference between the two systems, the kinetics of ROS generated by both the NADH oxidase and XOD systems were analysed by an electron spin resonance (ESR) spin trapping method using 5,5-dimethyl-1-pyrroline-*N*-oxide (DMPO), 5-(diethoxyphosphoryl)-5-methyl-pyrroline *N*-oxide (DEPMPO) and 5-(2,2-dimethyl-1,3-propoxy cyclophosphoryl)-5-methyl-1-pyrroline *N*-oxide (CYPMPO). As a result, two major differences in ROS kinetics were found between the two systems: (i) the kinetics of $^{\bullet}OH$ and (ii) the kinetics of hydrogen peroxide. In the NADH oxidase system, the interaction of hydrogen peroxide with each component of the enzyme system (NADPH, NADH oxidase and FAD) was found to generate $^{\bullet}OH$. In contrast, $^{\bullet}OH$ generation was found to be independent of hydrogen peroxide in the XOD system. In addition, the hydrogen peroxide level in the NADPH–NADH oxidase system was much lower than measured in the XOD system. This lower level of free hydrogen peroxide is most likely due to the interaction between hydrogen peroxide and NADPH, because the hydrogen peroxide level was reduced by ~90% in the presence of NADPH.**

*Keywords*: ESR spin trapping/hydrogen peroxide/NADPH oxidase/reactive oxygen species/xanthine oxidase.

*Abbreviations*: ESR, electron spin resonance; FAD, flavin adenine dinucleotide; NADPH, nicotinamide adenine dinucleotide phosphate; XOD, xanthine oxidase.

Reactive oxygen species (ROS) are generated from numerous sources *in vivo*. A number of different enzymes have been shown to generate ROS, including cytochrome P450s, various oxidases, peroxidases, lipoxygenases and dehydrogenases (*1–3*). The nicotinamide adenine dinucleotide (NADH)/nicotinamide adenine dinucleotide phosphate (NADPH) oxidase system and the xanthine oxidase (XOD) system are well-known systems that generate ROS. In phagocytic cells, for example, generation of ROS through the NADPH oxidase system is an important host defense mechanism involved in the destruction of invading microorganisms (*4–6*).

The microbicidal mechanism involves the initial phagocytosis of the pathogens, and the subsequent production and release of ROS and bactericidal proteins into the phagosomes. During the microbicidal response professional phagocytic cells produce a superoxide anion ($O_2^{-\cdot}$), a precursor of microbicidal oxidants (*7–9*), through the activation of NADH/NADPH oxidase. This enzyme catalyses the reduction of molecular oxygen to $O_2^{-\cdot}$ at the expense of NADPH as the electron donor in the phagocytes.

$$NADPH + 2O_2 \rightarrow NADP^+ + 2O_2^{-\cdot} + H^+$$

The $O_2^{-\cdot}$ subsequently reacts with itself, either spontaneously or under catalysis by superoxide dismutase (SOD), to form hydrogen peroxide and oxygen (*10*).

$$2O_2^{-\cdot} + 2H^+ \rightarrow H_2O_2 + O_2$$

ROS are also generated under ischaemic–reperfusion conditions. Under ischaemic conditions, hypoxanthine (HPX) is synthesized concomitantly with adenosine triphosphate (ATP)-consumption, and XOD is induced by xanthine dehydrogenase. XOD generates $O_2^{-\cdot}$ when acting on its substrates in the presence of oxygen (*10–12*), and the following pathway is postulated (*11*).

$$Enzyme - H_2 + 2O_2 \rightarrow Enzyme + 2H^+ + 2O_2^{-\cdot}$$
$$2O_2^{-\cdot} + 2H^+ \rightarrow O_2 + H_2O_2$$

In the reperfusion process following the ischaemia, ROS arise from $O_2^{-\cdot}$ generated by the enzymatic reaction of HPX–XOD. The resultant ROS cause cell damage and necrosis during reperfusion (*13*).

Kuppusamy and Zweier (*14*) speculated that XOD generates the highly reactive $^{\bullet}OH$ species via the

one-electron reduction of hydrogen peroxide at the flavin adenine dinucleotide (FAD) prosthetic group of the enzyme.

These two enzymes have often been used as an $O_2^{-\cdot}$ generation system. In our previous study, we observed that emission patterns of chemiluminescence, which was used to measure ROS generation, were different between the NADH oxidase system and the XOD system *in vitro* (E. Sato *et al.*, unpublished data), suggesting that the ROS generation pattern is different between the two oxidase systems. To characterize the difference between the two systems, an electron spin resonance (ESR) spin trapping method was used, and a colorimetric or spectrometric method was employed to analyse ROS generated by XOD and NADH oxidase.

## Materials and Methods

### Reagents

Reagents were purchased from the following sources: β-NADPH was from Oriental Yeast Co., Ltd. (Tokyo, Japan); FAD and SOD (from bovine erythrocytes, product no. S5395) were from Sigma-Aldrich (St. Louis, MO, USA); NADH oxidase was from Nacalai Tesque (Kyoto, Japan); catalase and *N*-(carboxymethylaminocarbonyl)-4,4′-bis(dimethylamino)-diphenylamine sodium salt (DA-64) were from Wako Pure Chemical Industries (Osaka, Japan); 5,5-dimethyl-1-pyrroline-*N*-oxide (DMPO) and XOD were from Labotec Co., Ltd. (Tokyo, Japan); diethylenetriamine-*N*, *N*, *N*′, *N*″, *N*″-pentaacetic acid (DTPA) was from Dojindo Laboratories (Kumamoto, Japan); 5-(diethoxyphosphoryl)-5-methyl-pyrroline *N*-oxide (DEPMPO) was from the Alexis Corporation (Lausen, Switzerland). 5-(2,2-dimethyl-1,3-propoxy cyclophosphoryl)-5-methyl-1-pyrroline *N*-oxide (CYPMPO) was synthesized according to the protocol described in a previous article (*15*). All other reagents used were of analytical grade.

### Detection of ROS by the ESR spin trapping method

ESR spin trapping determinations of ROS performed in this study were essentially identical to those described in our previous articles (*16*–*18*). The spin trap reagents DMPO, DEPMPO and CYPMPO were prepared at 4.45, 0.2 and 0.2 M in pure water, respectively. In the NADH oxidase system, a reaction mixture containing 50 µl of 2 mM NADPH in 0.1 M phosphate buffer (PB), 30 µl of 0.2 mM FAD in 0.1 M PB, 20 µl of 0.1 M PB, 30 µl of 0.1 M PB or DMSO, 20 µl of the spin trap reagent and 50 µl of 2 U/ml NADH oxidase in 0.1 M PB was prepared in a test tube. In the XOD system, a reaction mixture containing 50 µl of 2 mM HPX, 30 µl of 0.1 M PB or DMSO, 50 µl of 0.1 M PB, 20 µl of the spin trap reagent and 50 µl of 0.4 U/ml XOD in 0.1 M PB was prepared in a test tube. The mixtures were transferred to an ESR spectrometry cell, and the DMPO–OOH spin adduct (adduct from DMPO and the $O_2^{-\cdot}$) and the DMPO–OH spin adduct (adduct from DMPO and the $^{\bullet}OH$) were quantified 97 s after the addition of NADH oxidase or XOD. The measurement conditions of the ESR (JES-FA-100, JEOL, Tokyo) were as follows: field sweep, 330.5–340.5 mT; field modulation frequency, 100 kHz; field modulation width, 0.07 mT; amplitude, 500; sweep time, 2 min; time constant, 0.1 s; microwave frequency, 9.42 GHz; microwave power, 4 mW. The concentrations of the DMPO–OOH and DMPO–OH were determined from the peak area of the first signal of the DMPO–OOH and DMPO–OH spin adducts. In some experiments, the effects of ROS scavengers (SOD and catalase) were examined. The ROS scavengers, SOD and catalase, were prepared to 5,000 U/ml in pure water. In brief, a reaction mixture containing 50 µl of 2 mM NADPH in 0.1 M PB, 30 µl of 0.2 mM FAD in 0.1 M PB, 25 µl of 0.1 M PB, 25 µl of SOD or catalase solution or 0.1 M PB, 20 µl of 4.45 M DMPO and 50 µl of 2 U/ml NADH oxidase, or a reaction mixture containing 2 mM HPX, 55 µl of 0.1 M PB, 25 µl of SOD or catalase solution or 0.1 M PB, 20 µl of 4.45 M DMPO and 50 µl of 0.4 U/ml XOD was prepared in a test tube and mixed. The mixture was then transferred to an ESR spectrometry cell, and ESR analyses were performed 1, 3, 5 and 7 min following the addition of the NADH oxidase or XOD. ESR conditions were the same as those described above. In some experiments, DTPA was added to the reaction mixture to remove ferric salts. In brief, in the NADH oxidase system, a reaction mixture containing 50 µl of 2 mM NADPH in 0.1 M PB, 30 µl of 0.2 mM FAD in 0.1 M PB, 25 µl of 0.1 M PB, 25 µl of 10 mM DTPA in 0.1 M PB, 20 µl of the spin trap reagent and 50 µl of 2 U/ml NADH oxidase was prepared in a test tube. In the XOD system, a reaction mixture containing 50 µl of 2 mM HPX, 50 µl of 0.1 M PB, 30 µl of 10 mM DTPA in 0.1 M PB, 20 µl of the spin trap reagent and 50 µl of 0.4 U/ml XOD in 0.1 M PB was prepared in a test tube. The mixture was then transferred to an ESR spectrometry cell, and measured 1, 3, 5 and 7 min following the addition of the NADH oxidase or XOD. ESR conditions were the same as those described above.

### Detection of hydrogen peroxidase

The protocol used for the hydrogen peroxide assay involved using DA-64 as a coloring agent (Wako Pure Chemical Industries) and has previously been described (*19*). Briefly, in the NADH oxidase system, a reaction mixture containing 50 µl of 2 mM NADPH in 0.1 M PB, 30 µl of 0.2 mM FAD in 0.1 M PB, 45 µl of 0.1 M PB, 25 µl of a 5,000 U/ml SOD solution in pure water or 0.1 M PB and 50 µl of 2 U/ml NADH oxidase in 0.1 M PB was prepared in a test tube. In the XOD system, a reaction mixture containing 50 µl of 2 mM HPX, 75 µl of 0.1 M PB, 25 µl of a 5,000 U/ml SOD solution in pure water or 0.1 M PB and 50 µl of 0.4 U/ml XOD in 0.1 M PB was prepared in a test tube. Each mixture was then added to 1,800 µl of a reaction solution consisting of 0.1 mM DA-64, 0.1 M PIPES buffer (pH 7.0), 0.5% Triton X-100 and horse radish peroxidase (1 U/ml), and the resultant mixture was incubated for 5 min at 37°C. After incubation, the optical density at 727 nm was read (U-2010, Hitachi High-Tech Fielding Corporation, Tokyo). The concentrations of hydrogen peroxide were determined using a calibration curve, in which known concentrations of hydrogen peroxide were used as standards to generate the calibration curve.

### Quantitative assay of ROS

The spin concentrations of DMPO–OOH and DMPO–OH were determined using a previously described method (*16*, *20*). Briefly, the double integrals of DMPO–OOH or DMPO–OH signals were compared with those of a 20 µM TEMPOL standard measured under identical settings to estimate the concentrations of DMPO–OOH or DMPO–OH.

### Reactivity of the components of the NADH oxidase system with hydrogen peroxide

The reactivity of components of the NADH oxidase system (NADPH, NADH oxidase and FAD) with hydrogen peroxide was analysed by the ESR spin trapping method for free radicals and the colorimetric assay for hydrogen peroxide using DA-64. Each component of the NADH oxidase system was prepared in 0.1 M PB. In the ESR analysis, hydrogen peroxide was mixed with NADPH, NADH oxidase or FAD to a final concentration of 14.1 µM for hydrogen peroxide, and 0.5 mM for NADPH, 0.5 U/ml for NADH oxidase or 0.05 mM for FAD. DMPO–OOH and DMPO–OH were determined as described above (refer to 'Detection of ROS by the ESR spin trapping method' section). In the colorimetric analysis, a reaction mixture containing the same reagents as described above without DMPO was prepared. The concentrations of hydrogen peroxide were determined as described above (refer to the 'Detection of hydrogen peroxidase' section).

### Spectrophotometric analysis of the reaction between NADPH and hydrogen peroxide

The absorption spectra of NADPH with and without hydrogen peroxide were measured by a spectrophotometer (U-2010, Hitachi High-Tech Fielding Corporation, Tokyo). The solution containing 250 µl of 0.2 mM NADPH in 0.1 M PB, 625 µl of 0.1 M PB and 125 µl of 0.1 M PB or 10 µM hydrogen peroxide was prepared in a test tube. The mixture was transferred to a quartz cell, and the absorption spectrum at wavelength from 200 to 500 nm was monitored.

### Reactivity of the components of XOD system with superoxide anion radical

To examine which component (HPX or XOD) is involved in the reaction with $O_2^{-\cdot}$ to generate $^{\bullet}OH$ in the XOD system, each

component of the XOD system was added to the NADH oxidase system. In brief, a reaction mixture containing 50 µl of 2 mM NADPH in 0.1 M PB, 30 µl of 0.2 mM FAD in 0.1 M PB, 50 µl of 0.1 M PB or 2 mM HPX in 0.1 M PB or 0.4 U/ml XOD in 0.1 M PB, 20 µl of 4.45 M DMPO and 50 µl of 2 U/ml NADH oxidase in 0.1 M PB was prepared in a test tube. The mixture was then transferred to an ESR spectrometry cell, and ESR analyses were performed 1, 3, 5, 7, 9 and 11 min following the addition of the NADH oxidase. ESR conditions were the same as those described above.

## Results

### *Evaluation of the superoxide anion and the hydroxyl radical generated in NADH oxidase and XOD systems by the ESR spin trapping method*

Free radical generation from NADH oxidase in the presence of a substrate NADPH and from XOD in the presence of a substrate HPX was analysed using the ESR spin trapping method. Time course changes in the ESR spectra obtained from the NADH oxidase and XOD systems are shown in Figs 1 and 2, respectively. Three types of spin trap reagents DMPO, DEPMPO and CYPMPO were used to detect free radicals. Figs 1a and 2a present ESR spectra using DMPO. The spin adducts, DMPO–OOH and DMPO–OH, were assigned by hyperfine coupling constants (hfcc). The hfcc of DMPO–OOH were $a_H = 1.41$, $a_{H\beta} = 1.14$ and $a_{H\gamma} = 0.13$ mT, and the hfcc of DMPO–OH were $a_H = a_N = 1.49$ mT, which coincide with previously reported values (*21*). The concentrations of the DMPO–OOH and DMPO–OH at 97 s following the addition of NADH oxidase were 24.3 and 1.7 µM, respectively, and following the addition of XOD were 12.5 and 1.4 µM, respectively. Figs 1b and 2b show ESR spectra using DEPMPO obtained from the NADH oxidase reaction and the HPX–XOD reaction, respectively. The spin adducts DEPMPO–OOH and DEPMPO–OH were assigned by hfcc. DEPMPO–OOH has two kinds of hfcc, because DEPMPO consists of diastereomers. The hfcc values of DEPMPO–OOH were $a_P = 5.15$, $a_N = 1.32$, $a_H = 1.19$, $a_P = 4.88$, $a_N = 1.32$ and $a_H = 1.05$ mT. The hfcc values for DEPMPO–OH were $a_P = 4.70$, $a_N = 1.41$ and $a_H = 1.32$ mT, which coincide with previously reported values (*15*, *22*). The ESR spectra using CYPMPO were very similar to those using DEPMPO (data not shown). The spin adduct of CYPMPO has two kinds of hfcc because CYPMPO consists of diastereomers. The hfcc values of CYPMPO–OOH were $a_P = 5.08$, $a_N = 1.32$, $a_H = 1.03$, $a_P = 5.2$, $a_N = 1.28$ and $a_H = 1.12$ mT, whereas for CYPMPO–OH the hfcc values were $a_P = 4.88$, $a_N = 1.4$, $a_H$ 1.22, $a_P = 5.04$, $a_N = 1.4$ and $a_H = 1.39$ mT, which coincide with the values of CYPMPO–OOH and CYPMPO–OH adducts previously reported (*15*, *23*). The ESR signals of these spin adducts were analysed by isotropic simulation (JEOL). The $O_2^{-\cdot}$ adducts and the $^{\bullet}OH$ adducts of DEPMPO and CYPMPO are clearly identified by their centre signals because these signals do not overlap (*23*, *24*). To check the interference with an ESR signal derived from the spin trap, ESR analysis of each spin trap solution was conducted. As a result, no signals were detected when DEPMPO and CYPMPO solutions were analysed, and only a weak signal with negligible intensity was detected when a DMPO solution was analysed (data not shown). According to the time course changes in the ESR signals using DMPO in the NADH oxidase system (Fig. 1a), the signal intensity representing DMPO–OOH dramatically decreased, whereas the signal representing DMPO–OH gradually decreased over time following the addition of NADH oxidase. Conversely, in the XOD system the signal intensity representing DMPO–OH gradually increased, whereas the signal representing DMPO–OOH gradually decreased over time following the addition of XOD (Fig. 2a). From the results of ESR spectra using DEPMPO and CYPMPO, the yields of the spin adducts of $^{\bullet}OH$ obtained from the two spin traps were similar to that of DMPO, and the spin adducts of $O_2^{-\cdot}$ from the two spin traps were slightly different from that of DMPO. As shown in Figs 1 and 2, the signal arising from DEPMPO–OOH did not disappear until 7 min, possibly because of the longer half-lives of the $O_2^{-\cdot}$ adducts of DEPMPO (68 min) as compared with that of DMPO (1 min) (*15*). A similar result was observed for the signal arising from CYPMPO–OOH (data not shown). The free radical generation pattern in the XOD system determined by the ESR spin trapping method using DMPO in the present study was coincident with previously reported results (*14*). Although DEPMPO and CYPEMPO react with $O_2^{-\cdot}$ with a rate constant superior to DMPO and the corresponding spin trapped adducts have longer half-lives

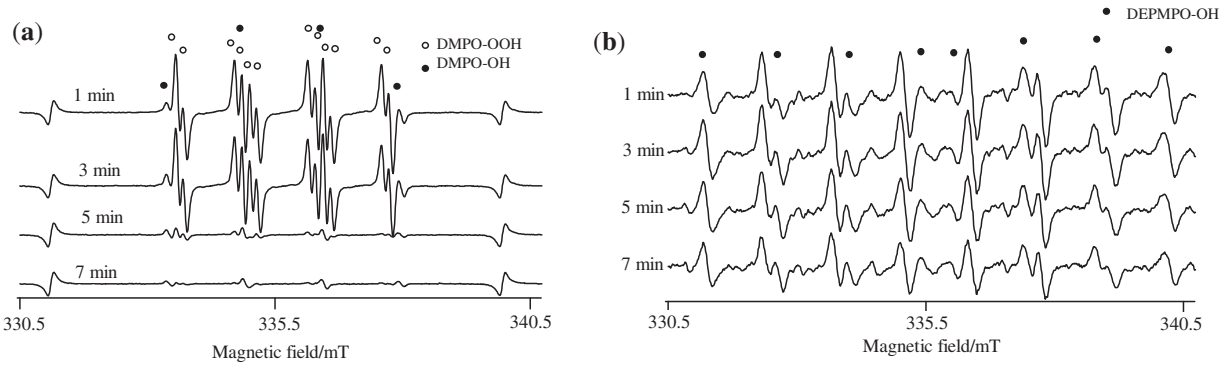


**Fig. 1** Time course changes in the ESR signals of DMPO adducts (a) and DEPMPO adducts (b) formed in the NADH oxidase system. Open circles and closed circles indicate signals derived from $O_2^{-\cdot}$ spin adducts and $^{\bullet}OH$ spin adducts, respectively. ESR analyses were performed 1, 3, 5, 7 min following the addition of the NADH oxidase.

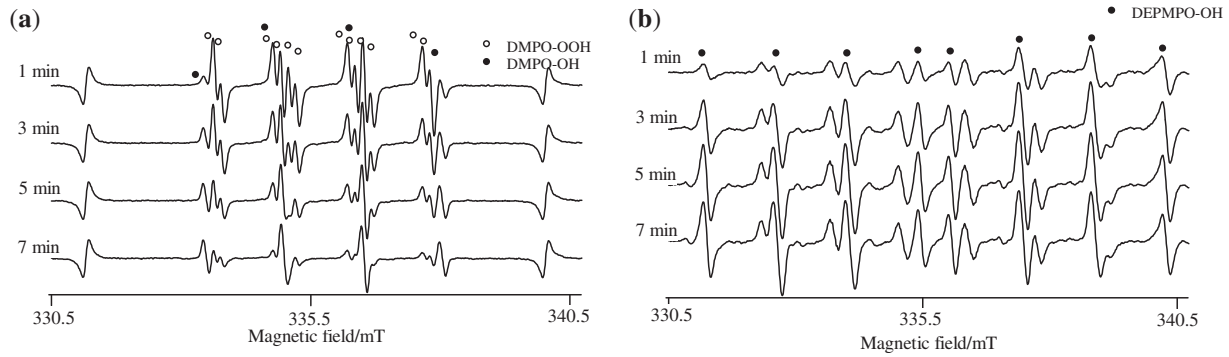


**Fig. 2** Time course changes in the ESR signals of DMPO adducts (a) and DEPMPO adducts (b) formed in the XOD system. Open circles and closed circles indicate signals derived from $O_2^{\cdot-}$ spin adducts and $^{\bullet}OH$ spin adducts, respectively. ESR analyses were performed 1, 3, 5, 7 min following the addition of the XOD.

than DMPO–OOH, the spin trap reagent DMPO was used in further experiments because DMPO–OH and DMPO–OOH are more distinguishable than the corresponding spin trapped adducts of DEPMPO and CYPMPO. Fig. 3 shows the spectra obtained in the presence of a potent $^{\bullet}OH$ scavenger, 1.92 M dimethyl sulphoxide (DMSO) in the NADH oxidase and XOD systems. When $^{\bullet}OH$ reacts with DMSO, it generates $^{\bullet}CH_3$ which can be potentially trapped by DMPO and therefore easily identified in both systems. The spectra show that the DMPO–$CH_3$ signal, which was assigned by hfcc ($a_H = 2.35$, $a_N = 1.64$ mT), but not the DMPO–OH signal was detected. ESR spectra obtained in the presence of 4.7 M methanol, a potent $^{\bullet}OH$ scavenger, also showed that the DMPO–$CH_3$ signal but not the DMPO–OH signal was detected (data not shown).

Furthermore, to study the possible involvement of $O_2^{\cdot-}$ in the generation of $^{\bullet}OH$, experiments were performed in the presence of SOD which is a scavenger against $O_2^{\cdot-}$. The ESR spectra obtained 1, 3, 5 and 7 min after the addition of NADH oxidase or XOD are shown in Fig. 4. In the both systems, SOD completely scavenged the $O_2^{\cdot-}$, hence no DMPO–OOH signal was observed. The DMPO–OH signal gradually increased with time in the NADH oxidase system, whereas the DMPO–OH signal did not changed between 1 and 7 min following the addition of XOD.

To determine whether the hydrogen peroxide is involved in the generation of $^{\bullet}OH$, experiments were performed in the presence of catalase which decomposes hydrogen peroxide. The ESR spectra obtained 1, 3, 5 and 7 min after the addition of NADH oxidase or XOD are shown in Fig. 5. In the NADH oxidase system, the addition of catalase decreased the signal intensity arising from DMPO–OH to an undetectable level 5 min after the addition of NADH oxidase, whereas the signal intensity arising from DMPO–OOH was not affected (Fig. 5a). In the XOD system, the kinetics of DMPO–OOH and DMPO–OH were the same as those in the absence of catalase (Figs 2a and 5b). Fig. 6 shows the spectra obtained in the presence of both SOD and catalase. In the NADH oxidase system, the DMPO–OOH and DMPO–OH signals completely disappeared when both SOD and catalase were present. In the XOD system, the DMPO–OOH signal completely disappeared; however, the signal intensity of the DMPO–OH adduct did not change between 1 and 7 min following the addition of XOD.

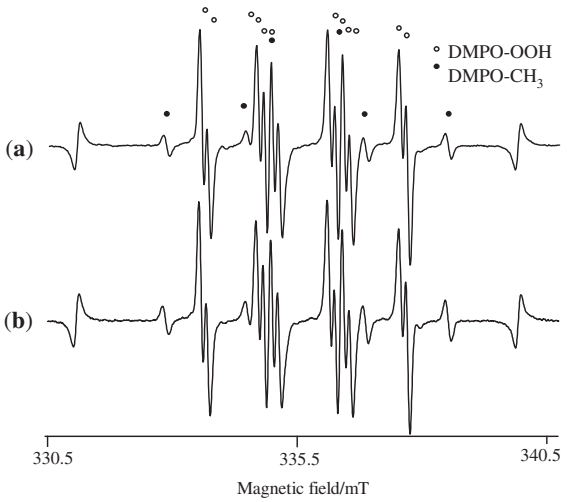


**Fig. 3** ESR signals of DMPO adducts formed in the NADH oxidase system (a) and the XOD system (b) in the presence of 1.92 M DMSO. Open circles and closed circles indicate signals derived from $O_2^{\cdot-}$ spin adducts of DMPO and $^{\bullet}CH_3$ spin adducts of DMPO, respectively.

### *Evaluation of hydrogen peroxide generation by a colorimetric assay*

The concentrations of the hydrogen peroxide generated from the NADH oxidase system and the XOD system 6 min after the addition of each oxidase are presented in Fig. 7. The concentration of hydrogen peroxide generated from the NADH oxidase system was 2.5 μM, whereas the concentration of hydrogen peroxide generated from the XOD system was 12.1 μM. To examine whether hydrogen peroxide generation is mediated by $O_2^{\cdot-}$ in the two oxidase systems, experiments were performed in the presence of SOD. Addition of SOD increased the concentration of hydrogen peroxide generated from the XOD system, whereas the levels of hydrogen peroxide generated from the NADH oxidase system did not change.

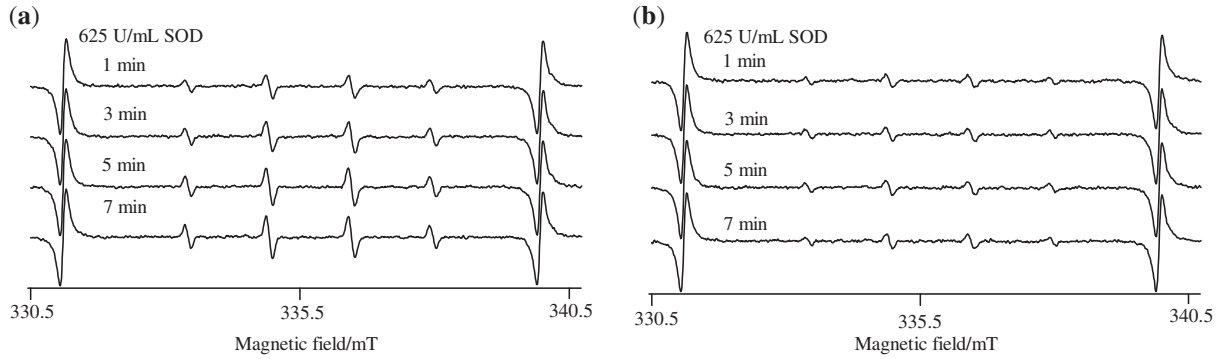


**Fig. 4** Time course changes in the ESR signals of DMPO adducts formed in the NADH oxidase system (a) and the XOD system (b) in the presence of 625 U/mL SOD. ESR analyses were performed 1, 3, 5, 7 min following the addition of the NADH oxidase (a) and XOD (b).

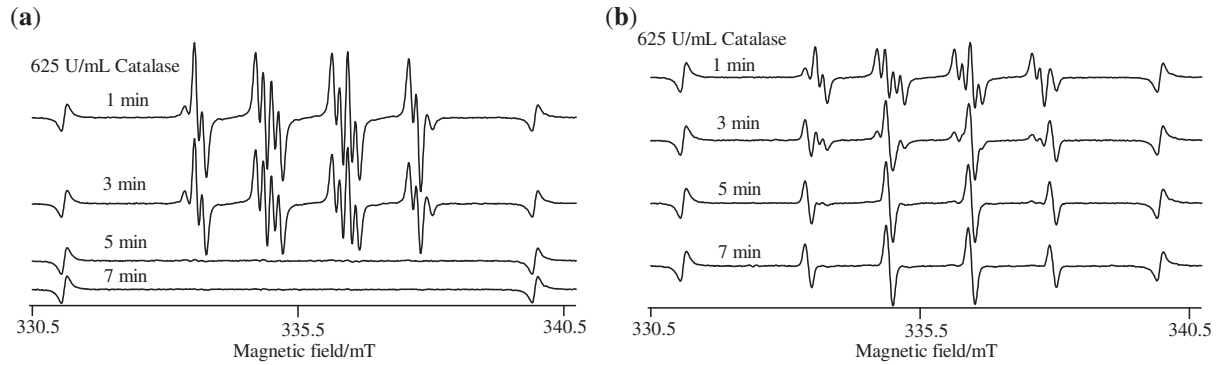


**Fig. 5** Time course changes in the ESR signals of DMPO adducts formed in the NADH oxidase system (a) and the XOD system (b) in the presence of 625 U/mL catalase. ESR analyses were performed 1, 3, 5, 7 min following the addition of the NADH oxidase (a) and XOD (b).

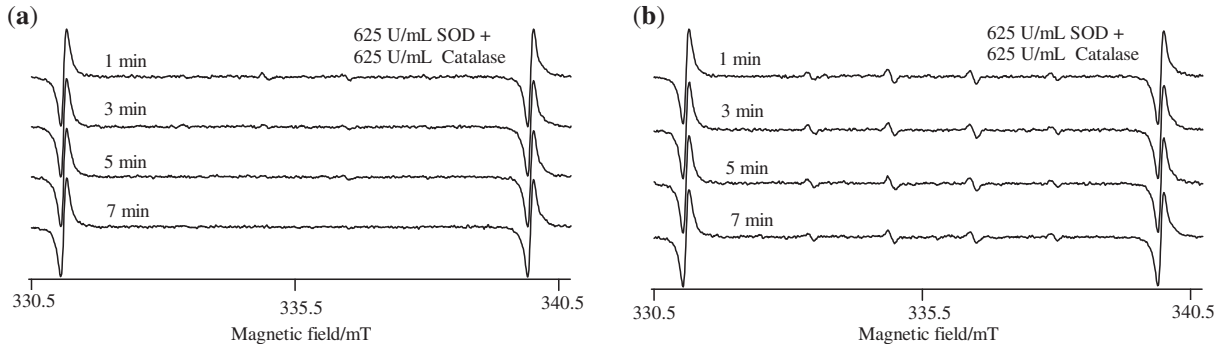


**Fig. 6** Time course changes in the ESR signals of DMPO adducts formed in the NADH oxidase system (a) and the XOD system (b) in the presence of both 625 U/mL SOD and 625 U/mL catalase. ESR analyses were performed 1, 3, 5, 7 min following the addition of the NADH oxidase (a) and XOD (b).

### *Reactivity of the components of the NADH oxidase system with hydrogen peroxide*

The amount of hydrogen peroxide generated from the NADH oxidase system was considerably lower when compared with the levels produced by the XOD system. Therefore, this raises the hypothesis that components of the NADH oxidase system react with hydrogen peroxide. Thus, changes in the concentrations of hydrogen peroxide were measured in the presence of NADPH, NADH oxidase or FAD. The concentration of hydrogen peroxide was not affected by the NADH oxidase and the FAD, whereas the levels drastically decreased in the presence of NADPH. The control solution was 14.1 μM hydrogen peroxide in 0.1 M PB. Measuring this standard solution by the DA-64 colorimetric method gave a concentration of 13.6 μM. The concentrations of hydrogen peroxide after the addition of the 0.5 mM NADPH and 0.5 U/ml NADH oxidase, and 0.05 mM FAD were 1.7, 13.5 and 13.7 μM, respectively. Furthermore, the generation of ROS under the same conditions was analysed by the ESR spin trapping method. In the presence of any of the components (NADPH, NADH oxidase and FAD), a small

amount of DMPO–OH was generated from hydrogen peroxide (data not shown). The concentrations of DMPO–OH generated from the reaction between hydrogen peroxide and NADPH, NADH oxidase and FAD were 0.23, 0.23 and 0.26 μM, respectively. In the absence of any of the components, 0.16 μM DMPO–OH was generated from hydrogen peroxide. Thus, the estimated total amount of DMPO–OH generated from the reaction between hydrogen peroxide and the components of the NADH oxidase system was calculated as follow: $0.16 + (0.23 - 0.16) + (0.23 - 0.16) + (0.26 - 0.16) = 0.4\,\mu M$.

### *Hydroxyl radical generation in the presence of hydrogen peroxide in the XOD system*

In a previous article it was proposed that the generation of $^{\bullet}OH$ in the XOD system is derived from hydrogen peroxide (*14*). To examine if the exogenous hydrogen peroxide induces the generation of $^{\bullet}OH$ in the XOD system, hydrogen peroxide amounts of 150, 75, 37.5 and 15 μM were added to the system. As a result, the DMPO–OH signal was not affected by the addition of any concentration of hydrogen peroxide (data not shown).

### *Spectrophotometric analysis of the reaction between NADPH and hydrogen peroxide*

To examine if NADPH reacts with hydrogen peroxide through an electron transfer from NADPH to hydrogen peroxide, the absorption spectrum from 200 to 500 nm was monitored because the absorption peak of NADPH is at 340 nm. However, addition of hydrogen peroxide to the NADPH solution did not affect the absorption spectrum of NADPH (data not shown).

### *Reactivity of the components of the XOD system with superoxide anion radical*

The component (HPX or XOD) of the XOD system was added to the NADH oxidase system to examine which component is involved in the generation of $^{\bullet}OH$ through the reaction with $O_2^{-\cdot}$ in the XOD system. The ESR spectra obtained 11 min following the addition of NADH oxidase are shown in Fig. 8. The yield of the DMPO–OH adduct obtained by the addition of XOD was ~50% higher than that by the addition of solvent, whereas it was not affected by the addition of HPX.

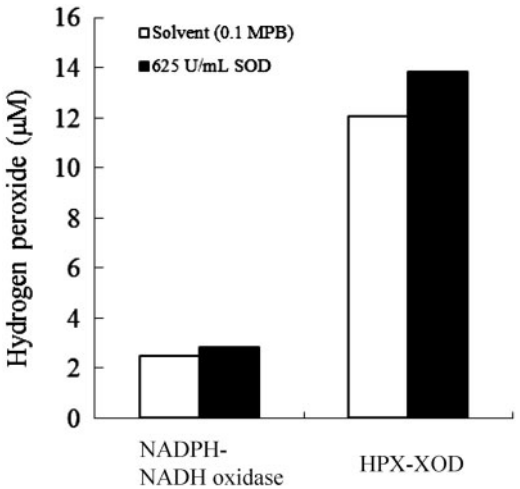


**Fig. 7 The concentrations of hydrogen peroxide generated from the NADH oxidase and XOD systems.** The white column indicates the concentration of hydrogen peroxide in the absence of SOD and the black column indicates the concentration of hydrogen peroxide in the presence of SOD. Each column represents the mean of triplicate determinations.

## Discussion

The results of the present study clearly showed that the kinetics of $^{\bullet}OH$ and $O_2^{-\cdot}$ are different between the NADH oxidase and the XOD systems (Figs 1 and 2). Three spin trap reagents DMPO, DEPMPO and CYPMPO were used to determine the radicals generated from the NADH oxidase and the XOD systems. Since there was the possibility that DMPO–OH is formed through decomposition or hydrolysis of DMPO–OOH, the following three experiments were conducted: (i) in addition to the conventional spin trap DMPO, DEPMPO and CYPMPO were used in the two enzyme systems, because the reaction rate between either DEPMPO or CYPMPO and $O_2^{-\cdot}$ is superior to DMPO, and their spin adducts have longer half-lives than that of DMPO; (ii) potent $^{\bullet}OH$ scavengers DMSO and methanol were used in the two enzyme systems to confirm the existence of a carbon-centered radical, because if $^{\bullet}OH$ exists, the radical reacts with DMSO or methanol to yield a carbon-centered radical and (iii) to check the existence of unwanted ferric salts possibly released from the glassware, DTPA was added to the two enzyme systems. From the results of (i), yields of spin adducts of $^{\bullet}OH$ obtained from the three spin traps were similar to each other, whereas the spin adducts of $O_2^{-\cdot}$ from the three traps were slightly different, possibly due to the longer half-lives of the adducts from DEPMPO and CYPMPO. From the results of (ii), the carbon-centered radical was found to be generated from the reactions between $^{\bullet}OH$ and the $^{\bullet}OH$ scavengers (Fig. 3) in both systems. From the results of (iii), the effect of DTPA on the ESR spectra was negligible, indicating that ferric salts did not play a role in the two enzyme systems examined. The combined results showed that $^{\bullet}OH$ was generated from the enzyme reactions but not from the decomposition of DMPO–OOH. In the experiments where the kinetics of $O_2^{-\cdot}$ and $^{\bullet}OH$ were compared between

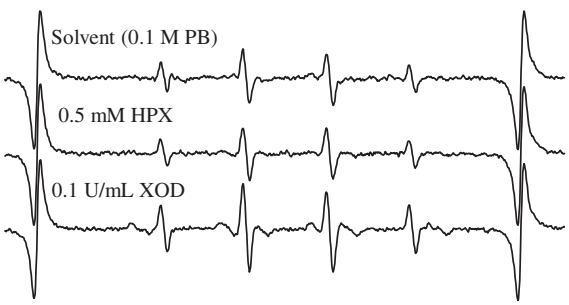


**Fig. 8** ESR signals of DMPO adducts formed in the NADH oxidase system obtained 11 min following the addition of NADH oxidase in the presence of solvent (0.1 M PB), 0.5 mM HPX or 0.1 U/ml XOD.

the NADH oxidase system and the XOD system, DMPO was used as a conventional spin trap because DMPO–OH and DMPO–OOH were more distinguishable than the corresponding spin trapped adducts of DEPMPO and CYPMPO. From the studies with ROS scavengers, SOD and catalase, two major differences were demonstrated in ROS kinetics between the NADH oxidase and the XOD systems (Figs 9 and 10). These differences were the kinetics of $^{\bullet}OH$ and hydrogen peroxide. In the NADH oxidase system, the results indicated that the $^{\bullet}OH$ species was derived from hydrogen peroxide, because the signal intensity of DMPO–OH increased with time in the presence of SOD, a potent scavenger against $O_2^{-\cdot}$ (Fig. 4a). SOD dismutates $O_2^{-\cdot}$ to hydrogen peroxide and $O_2$ as presented in the following reaction (*10*).

$$2O_2^{-\cdot} + 2H^+ \rightarrow H_2O_2 + O_2$$

Thus, scavenging of $O_2^{-\cdot}$ by SOD results in the generation of hydrogen peroxide, which is in turn converted to $^{\bullet}OH$ by a one electron reduction reaction. The presence of catalase, which is an enzyme that decomposes hydrogen peroxide, caused the complete disappearance of $^{\bullet}OH$ within 5 min (Fig. 5a), and a combination of SOD and catalase led to the disappearance of $^{\bullet}OH$ within 1 min (Fig. 6a). In the XOD system, that the results indicated that $^{\bullet}OH$ was derived at least in part from $O_2^{-\cdot}$ but not from hydrogen peroxide. As shown in Fig. 4b, the presence of SOD significantly decreased the amount of $^{\bullet}OH$, indicating that $^{\bullet}OH$ generation is associated with $O_2^{-\cdot}$. In contrast to the NADH oxidase system, catalase did not decrease $^{\bullet}OH$ (Fig. 5b), indicating that $^{\bullet}OH$ generation via the XOD system is independent of hydrogen peroxide. Consequently, as shown in Fig. 6b, the combination of SOD and catalase resulted in the observation of near identical ESR spectra as those spectra recorded for experiments with only SOD present (Fig. 4b).

From these results, the kinetics of hydrogen peroxide also appear to be different between the two enzyme systems. Thus, concentrations of hydrogen peroxide were determined. As shown in Fig. 7, the concentration of hydrogen peroxide in the NADH oxidase system was measured as 2.5 μM, whereas the concentration in the XOD system was 12.1 μM. The difference in the observed concentrations of hydrogen peroxide raised the hypothesis that the components of the NADH oxidase system interact with hydrogen peroxide. Indeed, in the experiment in which the addition of hydrogen peroxide to each component of NADH oxidase system, NADPH reduced the concentration of hydrogen peroxide, suggesting that the interaction of NADPH and hydrogen

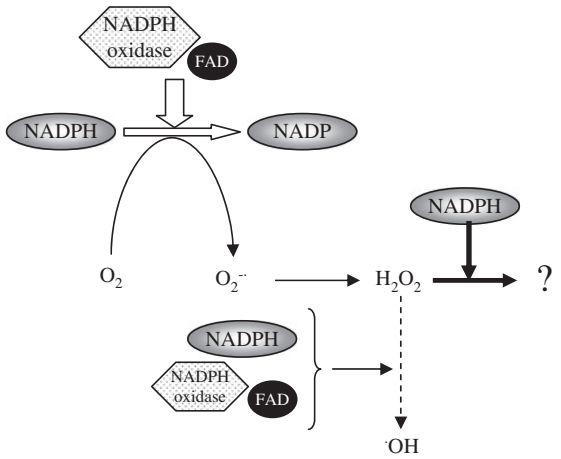


**Fig. 9 A schematic drawing of ROS kinetics in the NADH oxidase system.** $^{\bullet}OH$ is derived partially from a pathway indicated by the dashed line.

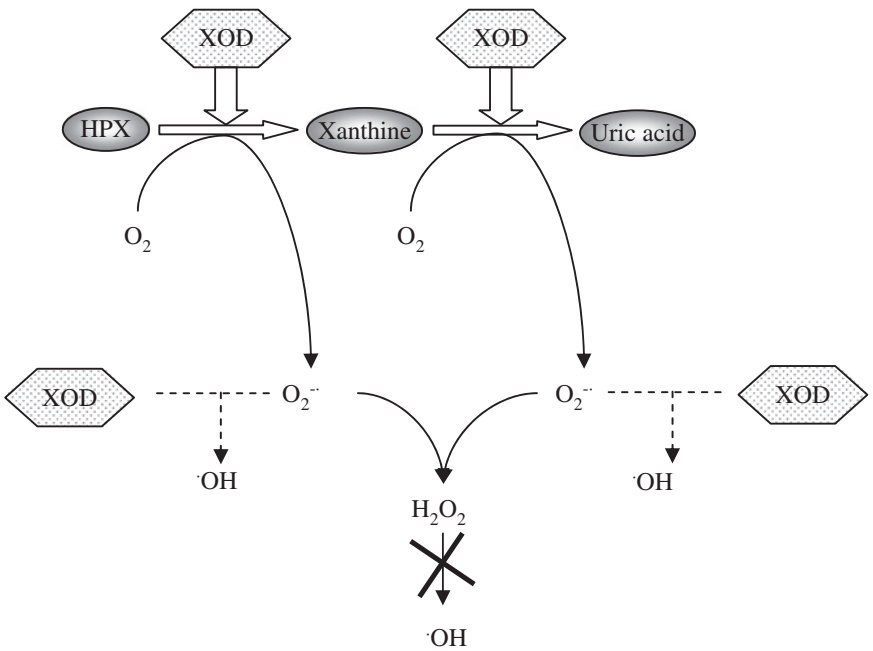


**Fig. 10 The schematic drawing of ROS kinetics in the XOD system.** $^{\bullet}OH$ is derived partially from a pathway indicated by the dashed line.

peroxide lowered the level of free hydrogen peroxide in the NADH oxidase system as compared with that in the XOD system. ESR analysis was performed to further examine if the components of the NADH oxidase system reacted with hydrogen peroxide to generate $^{\bullet}OH$. As a result, the total amount of $^{\bullet}OH$ from the reaction between each component (NADPH, NADH oxidase and FAD) and hydrogen peroxide was ~20% of the total amount generated in the NADH oxidase system. Therefore, 20% of the $^{\bullet}OH$ generated in the NADH oxidase system is likely to be derived from the reaction of hydrogen peroxide with the components of the NADH oxidase system.

With respect to how NADPH reduces the level of hydrogen peroxide, since absorption spectrum of NADPH was not affected by the addition of hydrogen peroxide, the reduction mechanism of hydrogen peroxide remains unclear and an issue to be elucidated. In the study of Kuppusamy *et al.* (*14*), exogenous hydrogen peroxide also increased the $^{\bullet}OH$ level in the xanthine–XOD system, suggesting that $^{\bullet}OH$ is derived from hydrogen peroxide. In the present study, however, exogenous hydrogen peroxide did not affect $^{\bullet}OH$ levels in the XOD system. Therefore, unlike the study by Kuppusamy *et al.* (*14*) it is strongly suggested that hydrogen peroxide is not associated with the generation or the kinetics of $^{\bullet}OH$ in the XOD system used in this study. From the result shown in Fig. 8 where the addition of XOD to NADH oxidase system increased the $^{\bullet}OH$ level, it is suggested that the interaction of XOD with $O_2^{-\cdot}$ is at least partly involved in the generation of $^{\bullet}OH$ in the XOD system. Taken these differences in the kinetics of $^{\bullet}OH$ and hydrogen peroxide between the NADH oxidase system and the XOD system into consideration, schematic drawings of ROS kinetics in the two enzyme reactions are illustrated in Figs 9 and 10. As shown in Fig. 9 where the ROS kinetics in the NADH oxidase system is illustrated, $O_2^{-\cdot}$ generated by the reaction of the NADH oxidase system is dismutated to form hydrogen peroxide. A fraction of hydrogen peroxide produced further reacts with NADPH and the other components of the NADH oxidase system, to generate $^{\bullet}OH$, the amount of which corresponds to ~20% of the total amount of $^{\bullet}OH$ produced in the system. However, the end products from the reaction between hydrogen peroxide and NADPH have not been identified. As shown in Fig. 10 where ROS kinetics in the XOD system is illustrated, $O_2^{-\cdot}$ is dismutated to form hydrogen peroxide. However, unlike the NADH oxidase system, $^{\bullet}OH$ formation is independent of hydrogen peroxide. A fraction of the $^{\bullet}OH$ produced is likely generated by the interaction of $O_2^{-\cdot}$ with XOD.

**Conflict of interest**
None declared.

## References


1. Brunk, U.T. and Terman, A. (2002) The mitochondrial-lysosomal axis theory of aging: accumulation of damaged mitochondria as a result of imperfect autophagocytosis. *Eur. J. Biochem.* **269**, 1996–2002
2. Caro, A.A. and Cederbaum, A.I. (2002) Role of calcium and calcium-activated proteases in CYP2E1-dependent toxicity in HEPG2 cells. *J. Biol. Chem.* **277**, 104–113
3. Gottlieb, R.A. (2003) Cytochrome P450: major player in reperfusion injury. *Arch. Biochem. Biophys.* **420**, 262–267
4. Aratani, Y., Kura, F., Watanabe, H., Akagawa, H., Takano, Y., Suzuki, K., Dinauer, M.C., Maeda, N., and Koyama, H. (2002) Relative contributions of myeloperoxidase and NADPH-oxidase to the early host defense against pulmonary infections with *Candida albicans* and *Aspergillus fumigatus*. *Med. Mycol.* **40**, 557–563
5. Espinosa, G.J. and Gutiérrez, M.C. (2003) The trapping of the OH radical by coenzyme Q. A teriretucal and experimental study. *J. Phys. Chem.* **107**, 9712–9725
6. El, B.J., Dang, P.M., Gougerot, P.M.A., and Elbim, C. (2005) Phagocyte NADPH oxidase: a multipomponent enzyme essential for host defense. *Arch. Immunol. Ther. Exp.* **53**, 199–206
7. Cross, A.R. and Jones, O.T. (1991) Enzymic mechanisms of superoxide production. *Biochim. Biophys. Acta* **1057**, 281–298
8. Babior, B.M. (1992) The respiratory burst oxidase. *Adv. Enzymol. Relat. Areas. Mol. Biol.* **65**, 49–95
9. Chanock, S.J., el Benna, J., Smith, R.M., and Babior, B.M. (1994) The respiratory burst oxidase. *J. Biol. Chem.* **269**, 24519–24522
10. McCord, J.M. and Fridovich, I. (1969) Superoxide dismutase. An enzymic function for erythrocuprein (hemocuprein). *J. Biol. Chem.* **244**, 6049–6055
11. Fridovich, I. (1970) Quantitative aspects of the production of superoxide anion radical by milk xanthine oxidase. *J. Biol. Chem.* **245**, 4053–4057
12. Kellogg, E.W. 3rd and Fridovich, I. (1975) Superoxide, hydrogen peroxide, and singlet oxygen in lipid peroxidation by a xanthine oxidase system. *J. Biol. Chem.* **250**, 8812–8817
13. Granger, D.N., Rutili, G., and McCord, J.M. (1981) Superoxide radicals in feline intestinal ischemia. *Gastroenterology* **81**, 22–29
14. Kuppusamy, P. and Zweier, J.L. (1989) Characterization of free radical generation by xanthine oxidase. Evidence for hydroxyl radical generation. *J. Biol. Chem.* **264**, 9880–9884
15. Kamibayashi, M., Oowada, S., Kameda, H., Okada, T., Inanami, O., Ohta, S., Ozawa, T., Makino, K., and Kotake, Y. (2006) Synthesis and characterization of a practically better DEPMPO-type spin trap, 5-(2,2--dimethyl-1,3-propoxy cyclophosphoryl)-5-methyl-1-pyrroline N-oxide (CYPMPO). *Free. Radic. Res.* **40**, 1166–1172
16. Niwano, Y., Sato, E., Kohno, M., Matsuyama, Y., Kim, D., and Oda, T. (2007) Antioxidant properties of aqueous extracts from red tide plankton cultures. *Biosci. Biotechnol. Biochem.* **71**, 1145–1153
17. Sato, E., Niwano, Y., Matsuyama, Y., Kim, D., Nakashima, T., Oda, T., and Kohno, M. (2007) Some dinophycean red tide plankton species generate a superoxide scavenging substance. *Biosci. Biotechnol. Biochem.* **71**, 704–710
18. Sato, E., Niwano, Y., Mokudai, T., Kohno, M., Matsuyama, Y., Kim, D., and Oda, T. (2007) A discrepancy in superoxide scavenging activity between the ESR-spin trapping method and the luminol chemiluminescence method. *Biosci. Biotechnol. Biochem.* **71**, 1505–1513
19. Sato, E., Kohno, M., and Niwano, Y. (2006) Increased level of tetrahydro-beta-carboline derivatives in

short-term fermented garlic. *Plant Foods Hum. Nutr.* **61**, 175–178
20. Kohno, M., Mizuta, Y., Kusai, M., Masumizu, T., and Makino, K. (1994) Measurements of superoxide anion radical and superoxide anion scavenging activity by electron spin resonance spectroscopy coupled with DMPOspin trapping. *Bull. Chem. Soc. Jpn.* **67**, 1085–1090
21. Buettner, G.R. (1987) Spin trapping: ESR parameters of spin adducts. *Free. Radic. Biol. Med.* **3**, 259–303
22. Frejaville, C., Karoui, H., Tuccio, B., Lemoigne, F., Culcasi, M., Pietri, S., Lauricella, R., and Tordo, P. (1994) 5-Diethoxyphosphoryl-5-methyl-1-pyrroline N-oxide (DEPMPO): a new phosphorylated nitrone for the efficient *in vitro* and *in vivo* spin trapping of oxygen-centered radicals. *J. Chem. Soc. Chem. Commun.* **15**, 1793–1794
23. Saito, K., Takahashi, M., Kamibayashi, M., Ozawa, T., and Kohno, M. (2009) Comparison of superoxide detection abilities of newly developed spin traps in the living cells. *Free. Radic. Res.* **43**, 668–676
24. Cheng, Q., Antholine, W.E., Myers, J.M., Kalyanaraman, B., Arner, E.S., and Myers, C.R. (2010) The selenium-independent inherent pro-oxidant NADPH oxidase activity of mammalian thioredoxin reductase and its selenium-dependent direct peroxidase activities. *J. Biol. Chem.* **285**, 21708–21723